

Article ID: 1006-8775(2011) 04-0418-12

PROGRESS OF MARINE METEOROLOGICAL OBSERVATION EXPERIMENT AT MAOMING OF SOUTH CHINA

HUANG Jian (黄 健)¹, CHAN Pak-wai (陈柏纬)²

(1. Guangzhou Institute of Tropical and Marine Meteorology, CMA, Guangzhou 510080 China; 2. Hong Kong Observatory, 134A Nathan Road, Kowloon, Hong Kong, China)

Abstract: The coastal area of southern China is frequently affected by marine meteorological disasters, and is also one of the key areas that influence the short-term climate change of China. Due to a lack of observational facilities and techniques, little has been done in this area in terms of operational weather monitoring and scientific research on atmospheric and marine environment. With the support of China Meteorological Administration (CMA) and Guangdong Meteorological Bureau (GMB), the Marine Meteorological Science Experiment Base (MMSEB) at Bohe, Maoming has been jointly established by Guangzhou Institute of Tropical and Marine Meteorology (GITMM) and Maoming Meteorological Bureau (MMB) of Guangdong Province after three years of hard work. It has become an integrated coastal observation base that is equipped with a complete set of sophisticated instruments. Equipment maintenance and data quality control procedures have been implemented to ensure the long-term, steady operation of the instruments and the availability of high quality data. Preliminary observations show that the data obtained by the MMSEB reveal many interesting features in the boundary layer structure and air-sea interaction in such disastrous weather as typhoons and sea fog. The MMSEB is expected to play an important role in the scientific research of disastrous weather related to marine meteorology.

Key words: Marine Meteorological Science Experiment Base; Maoming; observation; data quality control

CLC number: P732

Document code: A

doi: 10.3969/j.issn.1006-8775.2011.04.012

1 INTRODUCTION

The coastal area of southern China is one of the fastest growing economic development areas in China, and it is also one of the regions most affected by disasters related to marine meteorology. Disastrous weather such as typhoon, rainstorm, intense convective weather, strong wind over the seas, sea fog, huge sea wave and storm surge may bring about significant impact on the social and economic development in this area^[1-2]. Moreover, water vapor transport occurs over the southern China coast, which may lead to weather and climate anomaly over China. The water vapor originating from western Pacific, Indian Ocean and South China Sea is closely related to the large-scale, persistent drought/floods in this country^[3-6].

The boundary layer of the atmosphere is the region in which air-sea-land exchanges of mass and energy occur. The air-sea-land interactions over the coastal region of southern China may trigger and affect the occurrence of many different kinds of disastrous weather conditions related to marine

meteorology. At the same time, air-sea-land interactions in this region significantly affect energy and water vapor transport over the whole China. It would be beneficial to strengthen the study of air-sea-land interactions as well as boundary layer processes occurring in the southern coast of China. Such studies are expected to be helpful in revealing the mechanism of disastrous weather, understanding the pattern of short-term climate anomaly, and improving the prediction of weather and short-term climate. As such, they would be useful in terms of both scientific and practical significance^[7-8]. However, due to the lack of observational data, our understanding of the characteristics and evolution patterns of the air-sea interaction over South China Sea is very limited. In particular, the sea surface temperatures in the coastal regions have rather large fluctuations in the temporal scale and sharp gradients in the spatial scale. As a result, the air-sea interaction processes over the coastal regions are far more complicated and less understood than those occurring over the open sea^[9,10]. Understanding is more limited

Received 2010-05-21; **Revised** 2011-04-20; **Accepted** 2011-10-15

Foundation item: National Public Benefit Research Foundation (Meteorology) (GYHY200906008)

Biography: HUANG Jian, Senior Engineer, primarily undertaking research on marine meteorology.

Corresponding author: HUANG Jian, e-mail: hj@grmc.gov.cn

for such disastrous weather as landfalling typhoon, rainstorm, strong wind and sea fog, and the forecasting capability of which is lower than expected [11].

In the international community, there has been great emphasis on observational study of air-sea interaction and its relation with disasters associated with marine meteorology. A number of field studies have been conducted. For instance, in 1990, USA and USSR performed scientific experiments Tropical Cyclone Motion (TCM-90) and TYPHOON-90 over western North Pacific. ESCAP/WMO Typhoon Committee organized Special Experiment Concerning Typhoon Recurvature and Unusual Movement (SPECTRUM-90) for field studies of tropical cyclones. There are other field studies such as Climate Variability and Predictability (CLIVAR), Global Energy and Water Cycle Experiment (GEWEX) and World Weather Research Programme (WWRP). Moreover, Tropical Ocean Global Atmosphere Coupled Ocean-Atmosphere Response Experiment (TOGA COARE)^[9] and Coupled Boundary Layers and Air Sea Transfer Experiment (CBLAST)^[7, 8] take air-sea interaction as a major topic in the observational study. In China, the South China Sea Monsoon Experiment (SCSMEX) organized by China Meteorological Administration (CMA) in 1998 obtained large amount and wide variety of observational data of the atmosphere and the ocean, forming a concrete basis for the understanding of development, persistence and evolution of monsoon over South China Sea^[12]. In 2003, China Landfalling Typhoon Experiment (CLATEX) was organized with the objectives of understanding the changes in structure, intensity and movement of tropical cyclones before and after landfall, analyzing the characteristics of the boundary layer as well as the mechanism of persistence over land for landfalling tropical cyclones, and collecting their boundary layer data for the first time^[13]. Moreover, Ocean University of China carried out an observational study of air-sea interaction and characteristics of droplet spectrum of fog in Qingdao^[14]. Under the support of CMA and Guangdong Meteorological Bureau (GMB), the Guangzhou Institute of Tropical and Marine Meteorology (GITMM) has been dedicated towards the construction of marine meteorology observation network over the coastal areas of southern China since 2006. At the moment, the installation of the core observational station of the network, namely, the Marine Meteorological Science Experiment Base (MMSEB) at Bohe, Maoming, is basically completed. This paper introduces the meteorological instrumentation at MMSEB, the quality control procedures of the observational data, and the preliminary results of the analysis of the observations.

2 MAJOR FACILITIES AND OBSERVATIONAL INSTRUMENTS

The MMSEB, located at Dianbai county, Maoming city, Guangdong province ($21^{\circ} 27' 37''$ N, $111^{\circ} 19' 24''$ E), is shown in Fig. 1. This region experiences frequent occurrence of disastrous weather such as typhoon, rainstorm, strong wind and sea fog, as well as disastrous sea waves and storm surges^[11]. It is also a key area of the development of rain-bearing clouds in China^[3]. The MMSEB is mainly composed of Beishan observation station, an integrated observation platform over the sea, and a 100-m tall observation tower (Fig. 2a).

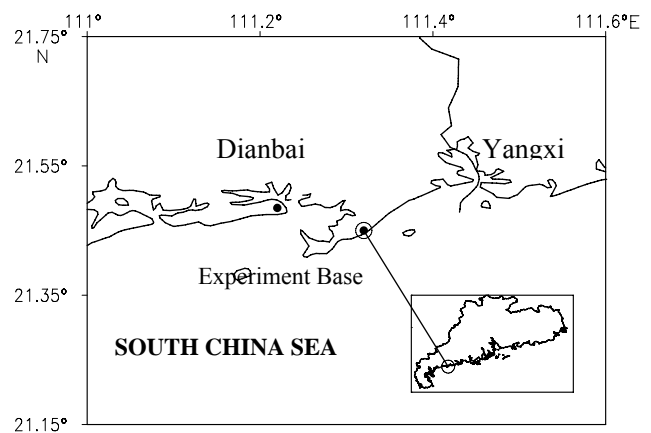


Fig. 1. The geographical location of the MMSEB (Experiment Base).

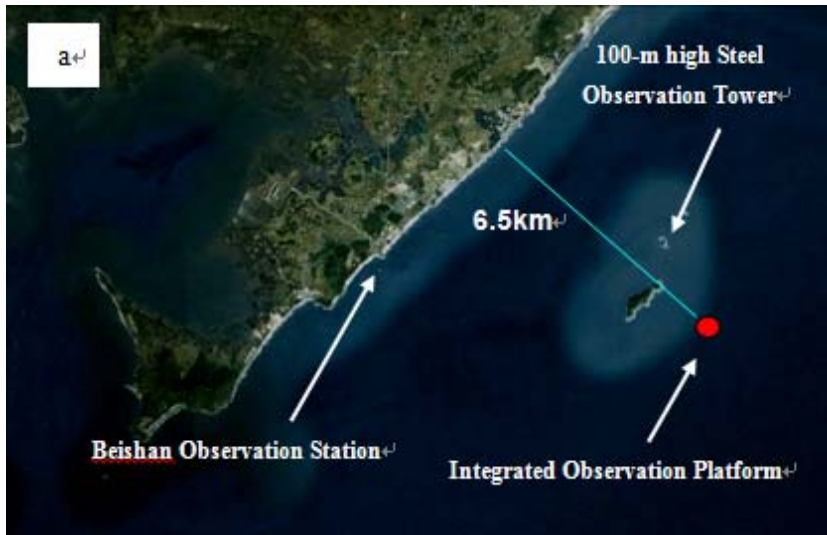
2.1 Beishan observation station

Beishan observation station is located at the coast of southern side of Liantou peninsula of Diancheng, Dianbai county. The coastline has northeast-southwest orientation, with the open ocean of South China Sea to the south, and hills with rather sparse vegetation to the north. In normal circumstances, the easterly and southerly winds from the sea are not much affected by local terrain, trees or buildings. According to the overall design strategy of the MMSEB, Beishan observation station is mainly used for measuring the vertical structure of the atmospheric boundary layer, meteorological elements near the surface, and elements related to the marine environment (Fig. 2b).

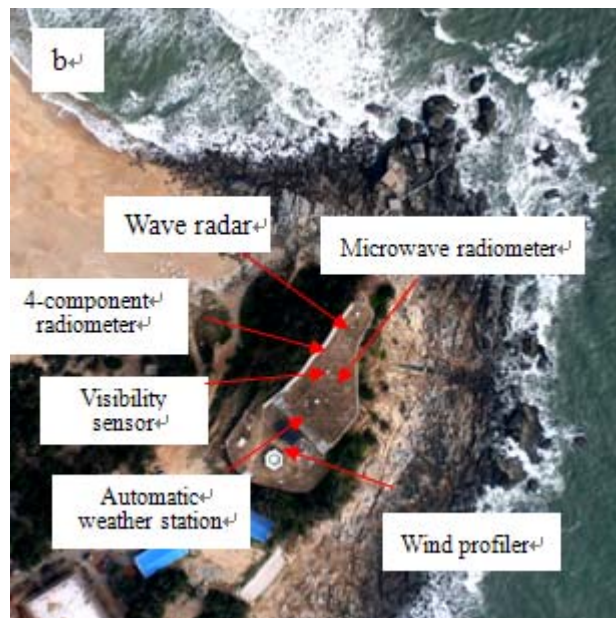
At present, the major observational facilities at Beishan observation station include: remote-sensing instruments such as a boundary-layer wind profiler and a microwave radiometer for continuous measurement of the vertical profiles of wind, temperature and humidity within the atmospheric boundary layer in high spatial and temporal resolutions; a GPS radiosonde and tethered sonde for in situ vertical profiling measurements on a need basis; surface observational equipment such as a four-component radiometer, an automatic weather station and a visibility sensor for measuring

upward/downward radiation flux for short and long-wave radiations, the net radiation flux, atmospheric visibility, wind direction, wind speed, air temperature, humidity, air pressure and precipitation. For ocean observation, the Beishan observation station mainly makes use of a wave-measuring buoy to collect ocean environmental data like sea surface temperature, wave height, wave direction and wave

period near the coastal areas. Moreover, to compensate the single-point measurement by a buoy only, the station also utilizes such remote-sensing instrument as a wave radar to measure the environmental parameters for sea waves and sea surface currents within 5 km from the coast. Table 1 presents a list of facilities installed at the Beishan observation station.



(a) Distribution of the observation facilities.



(b) Beishan observation station.



(c) Integrated observation platform.

(d) 100-m high steel observation tower).

Fig. 2. The major facilities and equipments of the MMSEB.

Table 1. The list of facilities at Beishan observation station.

| Name of equipment | Manufacturing place and model | Number | Observation parameters |
|---------------------------|--|--------------------|---|
| Wind profiler | Sumitomo WPR LQ-7 (with RASS) from Japan | One unit | Wind profiles, signal-to-noise ratio, turbulence structure function, etc. |
| Microwave radiometer | Radiometrics WP3000A from USA | One unit | Vertical profiles of temperature, water vapor and liquid water |
| Wave radar | WaMoS II wave detector from Germany | One unit | Parameters for sea waves and sea currents |
| Wave buoy | SBF3-1 wave buoy from China | One unit | Wave height, direction and period |
| 4-component radiometer | Kipp-zonen, CMP22/CGR4, CNR-1 from the Netherlands | One piece for each | Upward/downward short and long wave radiations |
| Automatic weather station | Vaisala MAWS301, MAWS201 from Finland | One piece for each | Six elements, including wind, temperature, humidity, pressure and precipitation |
| GPS sonde | Vaisala Digi-CORA MW31 from Finland | One unit | Vertical profiles of wind, temperature and humidity |
| Fog droplet spectrometer | DMT FM-100 from the USA | One unit | Droplet concentration and size for fog/ clouds |
| Visibility sensor | BELFORT M6000 from the USA | One unit | Scattering coefficient and visibility of the atmosphere |

2.2 Integrated observation platform over the sea

The integrated observation platform over the sea is built at a distance of 6.5 km away from the coast with the depth/height of 14 m/53 m below/above the sea surface. It is the first observation platform ever constructed for marine meteorology in China (Fig. 2c), which is mainly used for observing the processes related to the atmospheric boundary layer, the oceanic boundary layer and their interactions, and can be equipped with other observational facilities according to various scientific requirements. Its upper part is a steel tower of 25 m high. The lower part consists of

the base, supporting frames and a triangular platform. The observational components include a 25-m tower for observing air-sea fluxes and characteristics of the atmospheric boundary layer, a 10-m tower for measuring marine meteorological elements, and a submarine meteorological measuring facility. At present, the platform has been equipped with an eddy covariance observing system and a gradient observing system above the sea surface. Their major applications are collecting data such as air-sea flux, energy exchange and water vapor exchange. The submarine equipment includes temperature and salinity gradient

observation systems, a Doppler current profiler and a gravity-type sea wave detector, which are mainly used for observing marine boundary layer, sea wave and sea current. For the integrated observation platform (Fig. 2c), the facilities are shown in Table 2.

Table 2. The list of the facilities onboard the integrated observation platform.

| Name of the equipment | Manufacturing place and model | Number | Observation elements |
|---|---|--------------------|---|
| Sonic anemometer for wind and temperature measurements | Campbell CSAT3 from USA Gill R3-50 from UK | One piece for each | 3D wind speed, virtual temperature |
| Infrared CO ₂ /H ₂ O analyzers | Li-cor 7500 from USA | 2 units | Water vapor and CO ₂ |
| System for measuring the gradient of wind, temperature and humidity | RM. Young 05106 from USA Vaisala HMP45C from Finland | 5 levels | Gradient distribution of wind, temperature and humidity |
| Rain gauge | RM. Young from USA | 1 unit | Precipitation amount |
| thermal infrared sensor | Everest Interscience 4000.3ZL from USA | 1 unit | Sea skin temperature |
| Observation system for gradient of temperature and salinity | ALEC INFINITY-CTW from Japan | 4 levels | Gradient distribution of sea temperature and salinity |
| Acoustic Current Profiler | FLOWQUEST 1000 from USA | 1 unit | Profile of sea current speed |
| Gravity-type sea wave detector | FLOWQUEST from USA | 1 unit | Wave parameters |

2.3 100-m steel observation tower

The 100-m high steel observation tower is located on an island about 5 km from the coast. It is mainly used for observing air-sea flux and wind energy (Fig. 2d). The observation equipments include a Gill Wind MasterPro sonic anemometer for wind and temperature measurements, an observation system for wind and temperature gradients (with wind sensors at six levels of 10 m, 20 m, 40 m, 60 m, 80 m and 100 m, and temperature and humidity sensors at four levels of 10 m, 20 m, 40 m and 80 m). The observation elements include 3D wind speed, virtual temperature flux as well as the gradient distributions of wind direction, wind speed, air temperature and water vapor.

3 OPERATION OF MMSEB

Under the harsh environmental conditions of high temperature, high humidity and fog with high concentration of salt, it is common for the marine meteorology observation equipment to experience high fault rates, low quality of observation data and small amount of available measurements. Since there is just little work related to marine meteorology observation in China, negligible experience has been accumulated with regard to the maintenance of observation equipment and the quality control of measurements. Through experience gained in actual practice and making reference to the practice in other countries, the following measures have been taken at the MMSEB to ensure a long-term steady operation of

the meteorological observations.

3.1 Regular maintenance, calibration and replacement of faulty components of the facilities

The main challenge of field study over the sea and along the coast is the corrosion of the observation equipment due to sea salts. During the operation of the MMSEB, it is found that many instruments suffer from problems of short life-span and frequent failure. For instance, Vaisala HMP45C temperature and humidity sensor may work normally for about six months, and data collection computers could only run continuously for about one year. By making reference to the observation practices for surface meteorology, upper-air meteorology and ocean in other countries, we have devised plans for maintenance and calibration of observational equipments. The instruments are cleaned and maintained at regular intervals, and they are also checked constantly according to their related operation practices. As a result, the accuracy and reliability of the collected data have been guaranteed. Moreover, backup has been emphasized for those key components that break down frequently, so that the instrument can run continuously for sufficiently long time.

3.2 Performance of the observation equipment and the data quality

Since 2007, GITMM has performed verification many times on the key observation facilities such as the wind profiler, microwave radiometer and eddy

covariance system. The data collected by such facilities have been checked and assessed for completeness, reliability, consistency and normal variations. As a result, possible problems for such facilities can be discovered at an early time during routine operation and solved in a timely manner.

3.2.1 WIND PROFILER

The MMSEB has been equipped with WPR LQ7 boundary-layer type radar wind profiler developed jointly by Sumitomo Electric and Kyoto University in Japan. This profiler makes use of phased-array technology and Luneburg lens antenna for rather rapid scanning^[15]. During April–May 2007, a total of more than 50 GPS radiosondes were released, with about 42 sets of valid data collected. On this basis, the

performance of WPR-LQ7 wind profiler is evaluated.

Figure 3 gives the comparison results between the radar wind profiler and 42 measurements of wind direction and wind speed from GPS radiosondes. It is indicated that, below the height of 6000 m, the mean difference in wind direction is basically within $\pm 10^\circ$; the root-mean-square difference in wind direction is between 15–20°; the mean difference in wind speed is basically within ± 1 m/s; and the root-mean-square difference in wind speed is generally 1–2 m/s. In view of the differences between GPS radiosonde and wind profiler in terms of measurement methods as well as spatial and temporal sampling, it is inferred that the data from the two instruments are generally consistent with each other, and both can be used to give atmospheric information of the boundary layer.

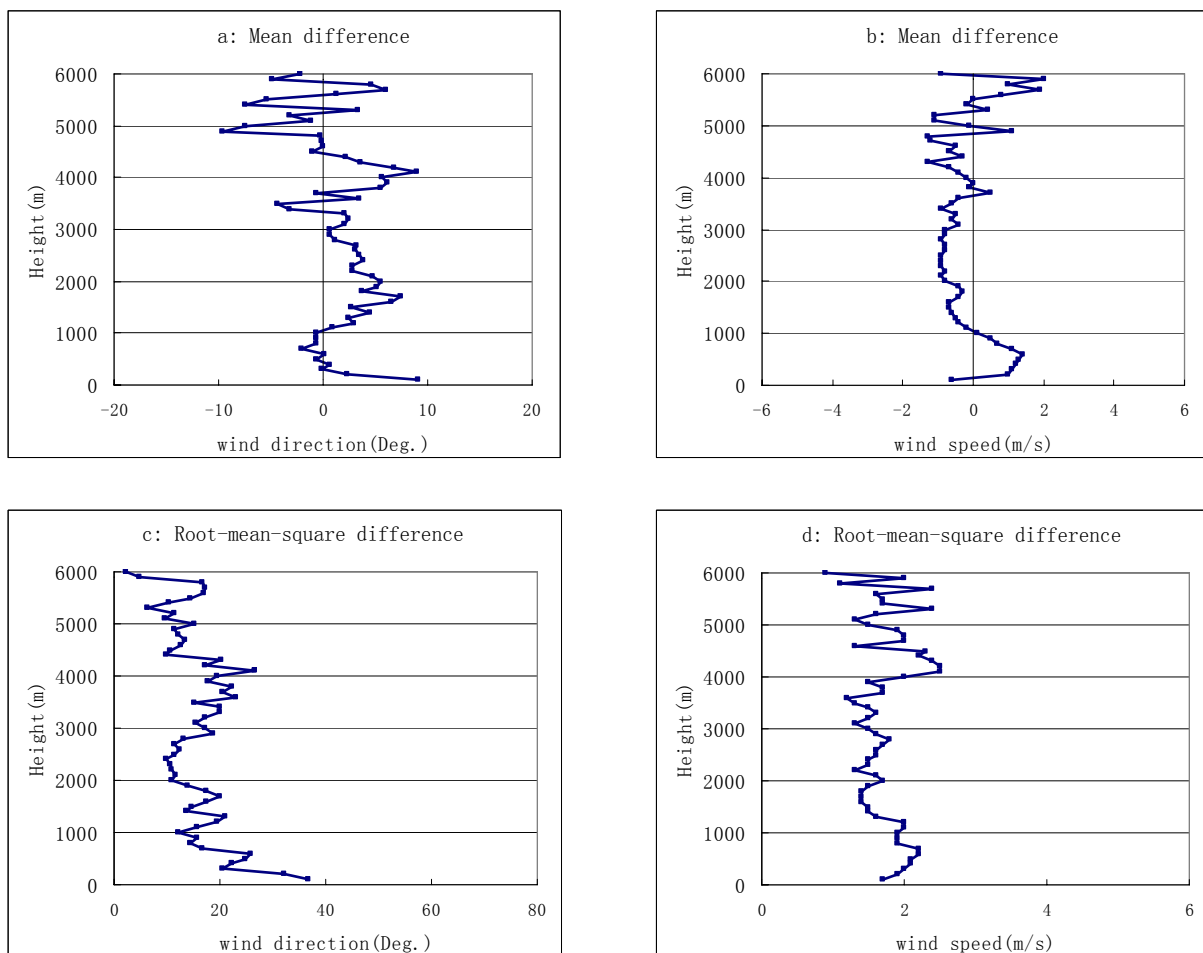


Fig. 3. Wind direction and wind speed from wind profiler and GPS radiosonde. (a) and (b) denote the mean difference in wind direction and wind speed, respectively. (c) and (d) denote the root-mean-square difference in wind direction and wind speed, respectively.

3.2.2 MICROWAVE RADIOMETER

WP3000A microwave radiometer is a passive remote-sensing instrument to retrieve atmospheric temperature and humidity profiles based on the measured brightness temperature of microwave radiation and the surface meteorological parameters. It

can provide data from the ground up to 10 km aloft in high temporal resolution^[16]. As a new remote-sensing method for atmospheric temperature, humidity and liquid water profiles, the radiometer has become more widely used both inside and outside the country^[17-19]. The radiometer uses a neural network method in the retrieval, namely, the input of the observed brightness

temperatures at the 35 microwave channels as well as the surface meteorological parameters (air temperature, air pressure and relative humidity), together with the historical observational data. The neural network in use is based on King's Park upper-air observation data of the Hong Kong Observatory during 1985–2004.

Using the GPS radiosonde as well as Yangjiang's upper-air sounding data during April–May 2007, the quality of the temperature and humidity data of the radiometer has been verified. This station is rather close to the MMSEB with a separation of about 80 km only. Comparison results show that the radiometer's temperature data are generally consistent with the GPS radiosonde as well as Yangjiang upper-air sounding data in the daytime. The differences between them are larger in the night time. On the other hand, though generally consistent in the general trend, the water vapor profile from the radiometer has a bias of 10% to 15% (Fig. 4).

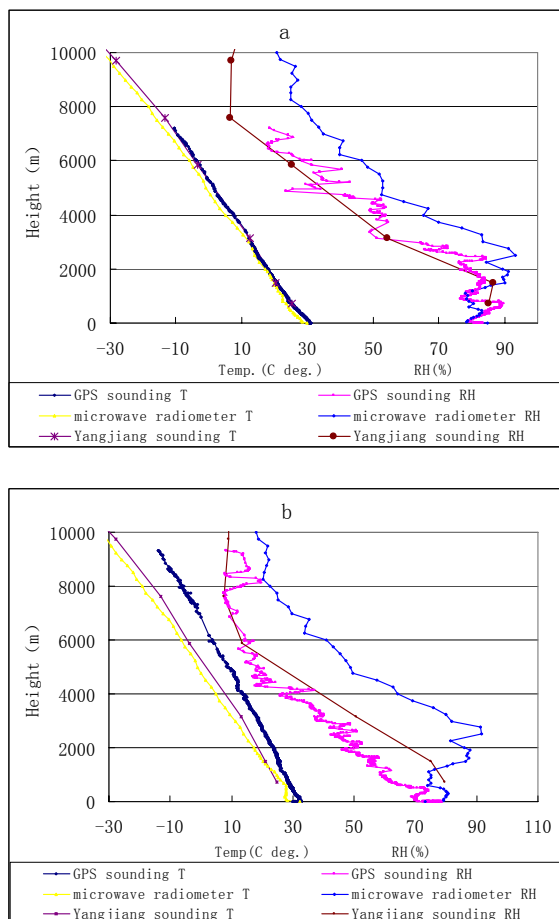


Fig. 4. The air temperature (T) and relative humidity (RH) observations from the microwave radiometer, GPS radiosonde, as well as Yangjiang's L-band upper-air ascent: (a) daytime, and (b) night-time.

3.2.3 EDDY COVARIANCE SYSTEM

Kolmogorov^[20] suggested that it is isotropic for turbulence associated with small-scale eddies within

the boundary layer, the power spectrum of which follows the $-2/3$ law, while the co-spectrum follows the $-4/3$ law. An analysis of the boundary layer atmospheric turbulence spectrum not only helps further understanding of the characteristics of the turbulent motion, but is also useful in examining the quality of the observational data. For this purpose, the time series data in a time interval of 30 minutes have been divided into 4096 segments, and Fast Fourier Transform (FFT) with Hamming filtering window is employed to calculate the turbulence spectrum and co-spectrum of the various fluctuating quantities^[21]. Fig. 5 shows the power spectra of vertical velocity, supersonic virtual temperature and water vapor. Fig. 6 gives the co-spectra between vertical velocity and horizontal wind speed, supersonic virtual temperature as well as water vapor.

It could be seen from Fig. 5 that the spectra of the various quantities have a similar peak at the low frequency region, with inertial subrange in the high frequency region. The power spectra of the various quantities basically follow the $-2/3$ law in the high frequency inertial subrange. The peaks of the spectra of the vertical velocity, temperature and humidity are located at about 0.01 Hz. But the peak value of humidity spectrum is larger than that of the temperature spectrum, which is consistent with the turbulence observations at other areas over the sea^[9]. Fig. 6 shows that the co-spectra for vertical velocity, supersonic virtual temperature as well as water vapor basically follow $-4/3$ law in the inertial subrange. However, its co-spectrum with horizontal wind speed has a slope smaller than $-4/3$. Since the observation site is close to the land, it may be influenced by the coastal terrain. As such, the underlying surface may not be in a completely uniform condition in terms of turbulence, and thus the spectra and co-spectra of the various quantities may not be exactly the same as the ideal situations.

3.3 Establishment of systems for data collection, processing and monitoring

In 2008, an integrated observational system was established at the MMSEB for data collection, processing and monitoring. It consists of two parts, namely, a database and a real-time data monitoring system. Among them, the observational database has a number of data interfaces. Data is transmitted through GPRS, local network as well as satellite communication from different locations and instruments for storage purpose. They are also processed in a centralized system. The real-time monitoring system keeps a close watch of the performance of the observation equipment, data communication facilities and data storage. It would alert the data management personnel for conducting timely recovery actions if the observational equipment

breaks down, there are anomalies with the data, or the data communication links fail to work.

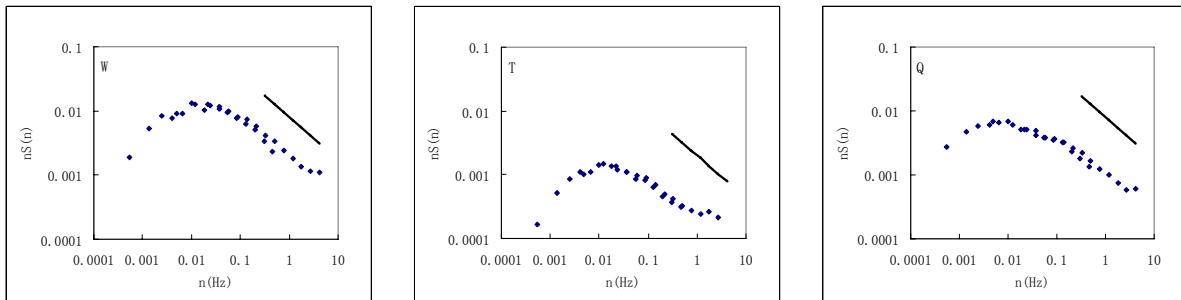


Fig. 5. Spectra of vertical velocity (W), water vapor (Q) and supersonic virtual temperature (T). The solid lines in the figures refer to $-2/3$ slopes.

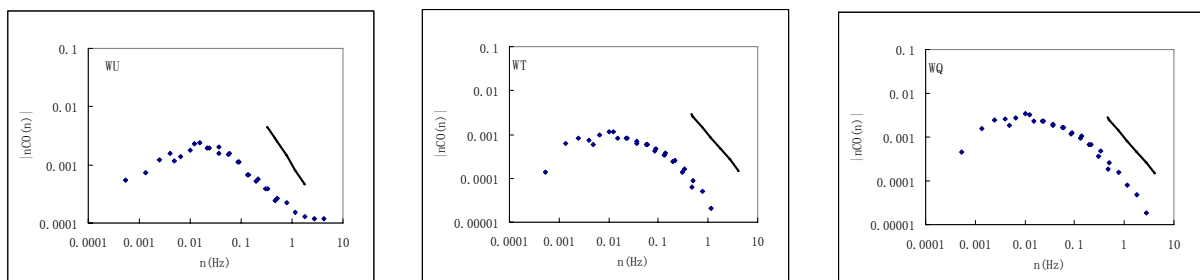


Fig. 6. Co-spectra between vertical velocity (W) and horizontal wind speed (U), supersonic virtual temperature (T) as well as water vapor (Q). The solid lines in the figures refer to the $-4/3$ slopes.

3.4 Quality control procedures for air-sea flux observations

The quality of the flux data depends on not only the performance of the observational equipment but also the method of processing the raw data. Different processing and correction methods may give rise to discrepancies of 10% or more for the final results^[21]. The processing of air-sea flux observation data basically follows the method recommended by FluxNet, including removal of data for abnormal sensor status, removal of apparently erroneous data by 4 times more than the standard deviation, co-ordinate transformation through planar fit, time-lag correction for H_2O and CO_2 , WPL correction for density fluctuations, correction for frequency loss, flux calculation (averaging over 30 minutes), examination of the steadiness of turbulence, and examination of turbulence development^[22]. Quality assurance procedures have also been implemented. Through all the new data processing procedures, the fluxes of sensible heat and latent heat are larger than those calculated by the original Campbell data processing method by 2.5% and 9.7% respectively.

It is well known that the water vapor content is higher in the air in marine environment. In the night-time, cooling by long-wave radiation usually leads to condensation of water droplets on the sensor heads when relative humidity is larger than 80%, resulting in anomalous recordings. To handle the water condensation problem in the night-time, the data quality control procedures not only include the

data removal during precipitation and the elimination of apparently erroneous data using the 5% threshold, but also implement the addition of automatic gain control (AGC) term in the raw data output from the sensor. AGC is used as an indicator for removing the anomalous readings in the real-time data stream. Comparing the raw data output and the data processed by the new method (Fig. 7), it could be seen that the use of the strengthened data quality control procedure helps remove the erroneous sensible heat and latent heat data arising from water condensation.

4 ANALYSIS OF OBSERVATIONS

Since 2007, the GITMM has conducted a series of field studies at the MMSEB under the sponsorship of CMA, National Science Foundation Fund, the national 973 scheme, and several scientific research programs. In this process, valuable data are obtained for such disastrous weather as landfalling typhoons, intense convective weather, rainstorms along the coast and sea fog. In this paper, typical weather conditions, namely, typhoon and sea fog are briefly discussed.

4.1 Variations in the structure of a landfalling typhoon

Severe typhoon Hagupit (0814) is one of the strongest typhoons making landfall over southern China in recent years. During the landfall, the 2-minute average wind speed reached 58 m/s, but the typhoon weakened rapidly over land^[23]. On the reason

of the rapid weakening, there have been suggestions in scientific research that it is related to the change from symmetric structure to asymmetric structure in the outer and inner cloud bands of the typhoon after

landfall^[24]. Asymmetric structure of the typhoon causes the latent heat release of the cumuli not concentrated near the typhoon centre, which then results in the weakening of the storm^[25].

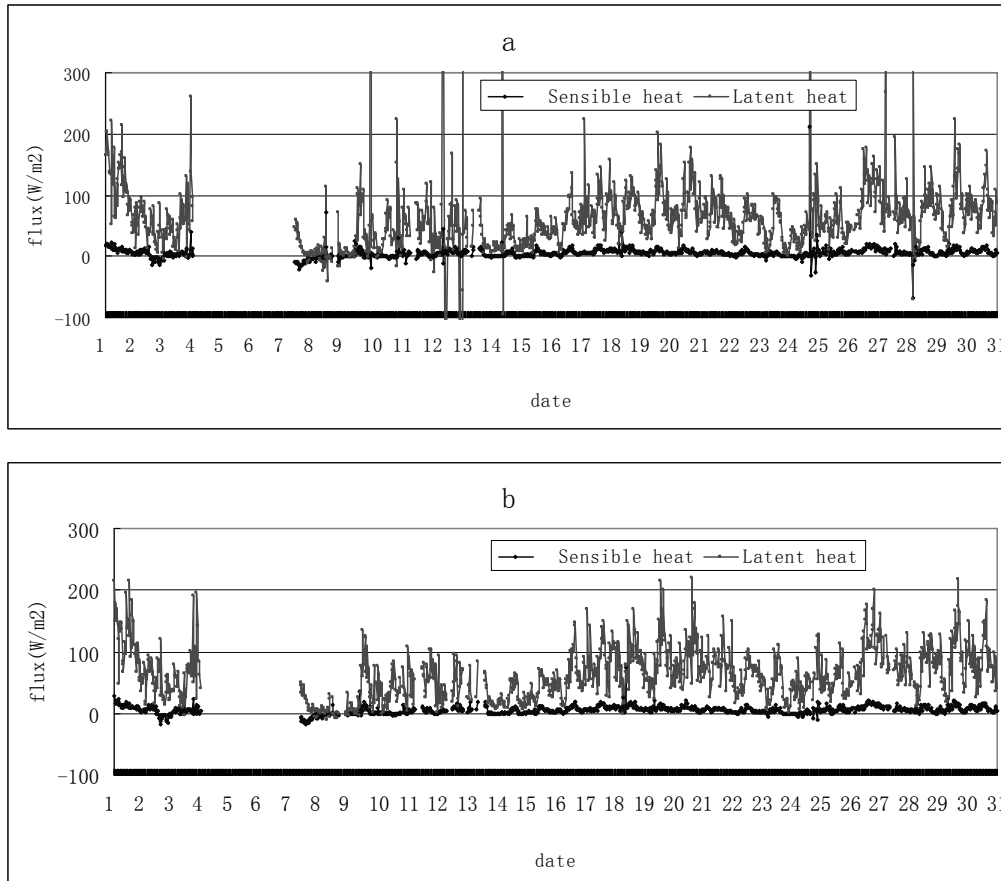


Fig. 7. (a) The sensible and latent heat processed by (a) the original method of Campbell Inc. and (b) the new method.

Using the high temporal resolution data from the wind profiler and radiometer at the base, we have plotted the cross-section of radial wind velocity and temperature along the line showed in Fig. 8 for Hagupit (Fig. 9). From the vertical distribution of the radial wind velocity, it could be seen that during landfall, the typhoon has a strong outflow between the heights of 1500 to 5000 m on the land side and inflow below 5000 m on the sea side (Fig. 9a). Asymmetric structure is apparent on the vertical structure of radial velocity. It is postulated that the difference in the surface layer between the land and the sea contributes to the asymmetry of the structure of the typhoon (Fig. 9b). The observational results in this typhoon case are consistent with the theory^[25].

4.2 Turbulent heat exchange in the sea fog

The sea fog along the coast of China is mainly advective cooling fog. During the evolution of this type of fog, the temperature inside the fog is higher than that of the sea surface. It is generally considered that the formation, development and persistence of

advective cooling fog are related to heat flux transport between the atmosphere and the cooler sea surface^[26, 27]. According to theoretical study, the long-wave radiative cooling at the fog top plays an important role in the evolution of advective cooling fog, especially in the vertical extension of the sea fog and deepening of the fog layer^[28, 29]. However, such a theory is not supported by observational data for many years.

On 24 to 25 March 2007, advective cooling fog was observed along the western coast of Guangdong, which indicates that, in the formation and dissipation stages, the fog layer is rather shallow and not deeper than 100 m; however, in the development and persistence stages, the fog layer reaches 600 m (Fig. 10). The heat flux data near the sea surface (Fig. 11) show that, in the formation and dissipation stages, the heat flux is rather small and the fog layer is mainly determined by the mechanical turbulence associated with wind shear; however, in the development and persistence stages, the heat transport near the sea surface increases as a result of long-wave radiative cooling near the fog top, and the vertical extension of

the fog layer occurs at about the same time as the increase of the heat flux^[30]. Such observations confirm the theoretical results of Rodhe^[28] and Wang^[29], which indicate the importance of long-wave radiative cooling at the fog top in the vertical extension of advective cooling fog. From the above observational cases, it is indicated that the MMSEB, equipped with sophisticated instruments, can capture many interesting features of the boundary layer structure of the landfalling tropical cyclone as well as the air-sea interaction in sea fog. Data of high temporal and spatial resolutions are obtained for operational monitoring and scientific research.

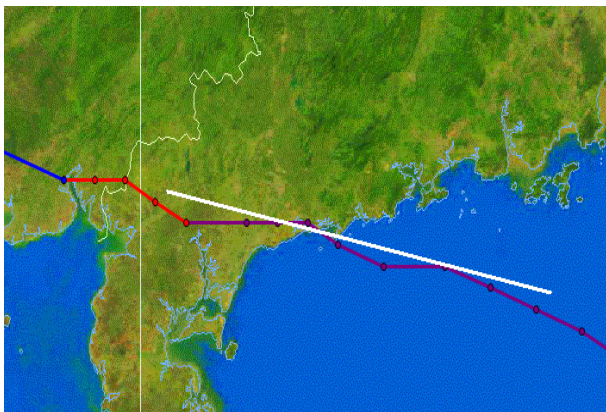


Fig. 8. The track of typhoon Hagupit (0814). The bold white line refers to the location of the vertical cross section in Fig. 9.

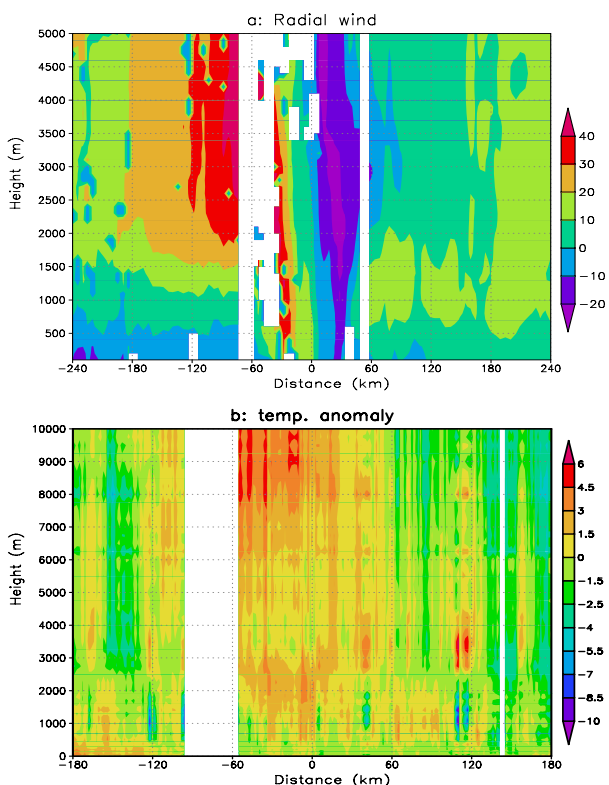


Fig. 9. The cross-section of (a) radial wind velocity (m/s) and (b) temperature (°C) during the landfalling of typhoon Hagupit (0814). The x-axis indicates the distance from the centre of the tropical cyclone.

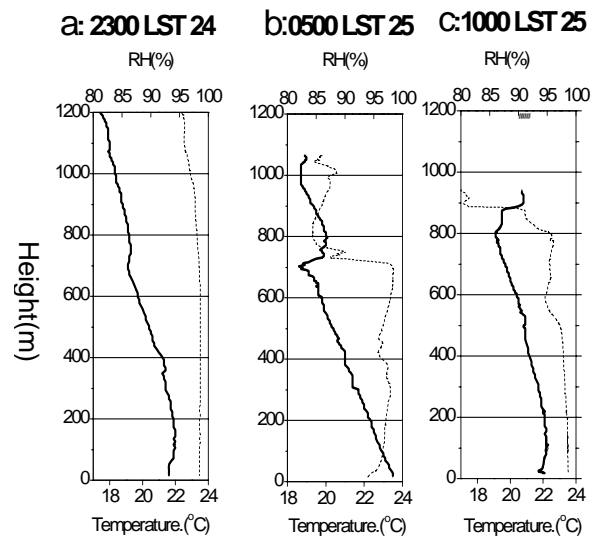


Fig. 10. Temperature (solid lines) and relative humidity profiles (dotted lines) in sea fog (a: observed at 2300 LST 24th; b: observed at 0500 LST 25th ; c: observed at 1000 LST 25th March 2007).

5 CONCLUSIONS

With the support of CMA and GMB, GITMM has taken great efforts in the past three years to preliminarily complete the construction of the MMSEB and put it into operational use. This paper introduces the major facilities of the MMSEB, the operation of the observation, and the analysis on typical cases of landfalling typhoon and sea fog.

(1) The MMSEB aims at observing the characteristics and evolution patterns of the boundary layer structure and air-sea-land interaction at times of disastrous weather conditions along the coast.

(2) Under the harsh conditions of high temperature, high humidity and fog with high salt content along the coast, the observation equipment may suffer from frequent breakdown, low data availability and poor data quality. A number of measures have been taken to effectively achieve the continuous, steady operation of the equipment and the long-term availability of high quality data, including regular maintenance, calibration as well as component replacement for the instruments; verification of the equipment and data quality; implementation of procedures for data checking; and the establishment of a synthetic system for data collection, processing and monitoring.

(3) From a preliminary analysis of observations in several cases, it can be seen that the data obtained by the MMSEB reveal many interesting features of the boundary layer structure and air-sea interaction in such disastrous weather as typhoons and sea fog. The MMSEB should be more valuable for operational weather monitoring and scientific research in the future.

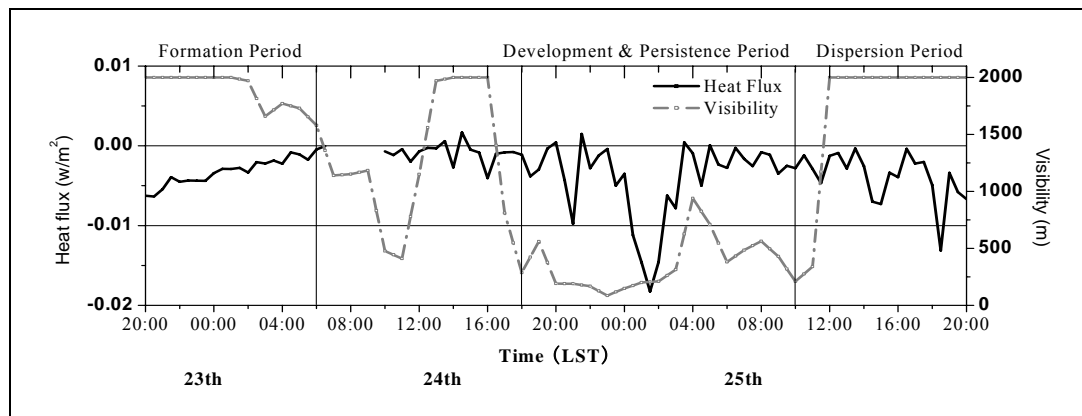


Fig. 11. Time series of turbulent heat flux and visibility in the sea fog for the period of 24th to 25th March 2007.

Acknowledgement: In drafting this manuscript, great effort has been made by CHEN Rong, WAN Qi-lin, LIANG Jian-yin, Yi YAN-ming, HUANG Hui-jun, MAO Wei-kang, LIAO Fei, Liu CHUN-xia, YUANG Jin-nan, ZHAO Zhong-kuo, BI Xue-yan, CHEN Yu-qun, DENG Hua and LI Shu-min of GITMM as well as LV Wei-hua, ZHAN Guo-wei, YANG Yong-quan of MMB.

REFERENCES:

- [1] YAN Jun-yue, CHEN Qian-jin, ZHANG Xiu-zhi et al. *Climates of China Adjacent Seas* [M]. Beijing: China Science Press (in Chinese), 1992.
- [2] LIN Liang-xun, co-authors. *Technical Guidance on Weather Forecasting in Guangdong Province* [M]. Beijing: China Meteorological Press (in Chinese), 2006.
- [3] WU Guo-xiong. Atmospheric transports and budgets of water vapor and their impacts on subtropical drought [J]. *Chin. J. Atmos. Sci.* (in Chinese), 1990, 14(1): 53-63.
- [4] HUANG Rong-hui, ZHANG Zhen-zhou, HUANG Gang, et al. Characteristics of the water vapor transport in East Asian monsoon region and its difference from that in South Asian monsoon region in summer [J]. *Chin. J. Atmos. Sci.* (in Chinese), 1998, 22(4): 460-469.
- [5] WANG D X, ZHOU W, YU X L, et al. Marine atmospheric boundary layers associated with summer monsoon onset over the South China Sea in 1998 [J]. *Atmos. Oceanic Sci. Lett.*, 2010, 3: 263-270.
- [6] HUANG Rong-hui, LI Chong-yin, WANG Shao-wu, et al. *On the Major Climate Disasters and Their Formation* [M]. Beijing: China Meteorological Press (in Chinese), 2003.
- [7] EDSON J, co-authors. The Coupled Boundary Layers and Air Sea Transfer Experiment in Low Winds [J]. *Bull. Amer. Meteor. Soc.*, 2007, 88: 341-356.
- [8] BLACK P G, Co-authors. Air sea exchange in hurricanes: Synthesis of observations from the Coupled Boundary Layer Air Sea Transfer experiment [J]. *Bull. Amer. Meteor. Soc.*, 2007, 88: 357-384.
- [9] WELLER R A, BRADLEY E F, LUKAS R. The interface or air-sea flux component of the TOGA Coupled Ocean-Atmosphere Response Experiment and its impact on future air-sea interaction studies [J]. *J. Atmos. Ocean. Tech.*, 2004, 21: 223-257.
- [10] WANG Dong-xiao, ZHANG Yan, ZENG Li-li, et al. Marine meteorology research progress of China from 2003 to 2006 [J]. *Adv. Atmos. Sci.*, 2009, 26(1): 17-30.
- [11] XU Xiao-feng, GU Jian-qun, LI Yong-ping. Series of weather disasters-Marine Meteorological Disasters [M]. Beijing: China Meteorological Press, 2009.
- [12] DING Yi-hui. *Water Vapor Budget in Monsoon Areas: Asia Monsoons* [M]. Beijing: China Meteorological Press (in Chinese), 1994.
- [13] CHEN Lian-shou, LUO Zhe-xian, LI Ying. Research advances on tropical cyclone landfall process [J]. *Acta Meteor. Sinica* (in Chinese). 2004, 62(2) : 541-549.
- [14] XU Jing-qi, ZHANG Zheng, WEI Hao. Measurement and analysis of droplet spectrum and liquid water content of sea fog [J]. *Transac. Oceanol. Limnol.* (in Chinese), 1994, 2: 174-178.
- [15] IMAI K, NAKAGAWA T, HASHIGUCHI H. Development of Tropospheric Wind Profiler Radar with Luneberg Lens Antenna (WPR LQ-7) [R]. *Sci. Tech. Rev.*, 2007, 64: 38-42.
- [16] WARE R, CARPENTER R, GULDNER J, et al. A multichannel radiometric profiler of temperature, humidity, and cloud liquid [J]. *Radio Sci.*, 2003, 38: 8079, doi:10.1029/2002RS002856.
- [17] KNUPP K R, COLEMAN T, PHILLIPS D, et al. Ground-based passive microwave profiling during dynamic weather conditions [J]. *J. Atmos. Ocean. Tech.*, 2009, 26: 1057-1073.
- [18] LIU Hong-yan, WANG Ying-chun, WANG Jing-li, et al. Preliminary analysis of the characteristics of precipitable water vapor measured by the ground-based 12-channel microwave radiometer in Beijing [J]. *Chin. J. Atmos. Sci.* (in Chinese), 2009, 33(2): 388-396.
- [19] CHAN P W, TAM C M. Performance and application of a multi wavelength, ground based microwave radiometer in nowcasting [C]// 9th Symposium on Integrated Observing and Assimilation Systems for the Atmosphere, Oceans, and Land Surface. San Diego: American Meteorological Society, 2005.
- [20] KOLMOGOROV A N. Dissipation of energy in a locally isotropic turbulence [J]. *Doklady Akad. Nauk SSSR*, 1941, 32: 141.
- [21] FINNIGAN J, CLEMENT J, MALHI R, et al. A reevaluation of long-term flux measurement techniques, Part I: Averaging and coordinate rotation [J]. *Bound. Layer Meteor.*, 2003, 107: 1-48.
- [22] FOKEN T. *Micrometeorology* [M]. Berlin: Springer, 2008.
- [23] HUANG Jian, LIANG Jian-yin, WAN Qi-lin et al. An observational study on the asymmetric structure of landfall tropical cyclone [J]. *J. Trop. Meteor.*, (in Chinese)(in press).
- [24] CHEN Lian-shou, XU Xiang-de, LUO Zhe-xian, et al. *Introduction to Tropical Cyclone Dynamics* [M]. Beijing: China Meteorological Press, 2002.
- [25] DUAN Yi-hong, WU Rong-sheng, YU Hui, et al. The role

of β -effect of planetary vorticity gradient and uniform current on the change in tropical cyclone intensity [J]. *Adv. Atmos. Sci.*, 2004, 21: 75-86.

[26] LEWIS J M, KORACIN D, REDMOND K T. Sea fog research in the United Kingdom and United States: a historical essay including outlook [J]. *Bull. Amer. Meteor. Soc.*, 2004, 75: 395-408.

[27] GULTEPE I, TARDIF R, MICHAELIDES S C, et al. Fog research: A review of past achievements and future perspectives [J]. *Pure Appl. Geophys.*, 2007, 164: 1121-1159.

[28] RODHE B. The effect of turbulence on fog formation [J]. *Tellus*, 1962, 14: 49-86.

[29] WANG Bin-hua. *Sea Fog* [M]. Beijing: China Ocean Press, 1985.

[30] HUANG Jian, WANG Bin, ZHOU Fa-xiu et al. Turbulent heat exchange in a warm sea fog event on the coast of South China [J]. *Chin. J. Atmos. Sci. (in Chinese)*, 2010, 34(4): 715-725.

Citation: HUANG Jian and CHAN Pak-wai. Progress of marine meteorological observation experiment at Maoming of South China. *J. Trop. Meteor.*, 2011, 17(4): 418-429.